

Squeezing Effect in the Gouy Phase of Matter Waves

Thiago M. S. Oliveira,¹ Lucas S. Marinho ¹, F. C. V. de Brito,^{2,*} Marcos Sampaio,³ and Irismar G. da Paz ^{1,†}

¹*Departamento de Física, Universidade Federal do Piauí,*

Campus Ministro Petrônio Portela, 64049-550, Teresina, PI, Brazil

²*Institute of Physics, Faculty of Physics, Astronomy and Informatics,*

Nicolaus Copernicus University in Toruń, ul. Grudziądzka 5, 87-100 Toruń, Poland

³*Centro de Ciências Naturais e Humanas, Universidade Federal do ABC,*

Avenida dos Estados 5001, 09210-580 Santo André, São Paulo, Brazil

(Dated: April 22, 2025)

We investigate the Gouy phase emerging from the time evolution of confined matter waves in a harmonic potential. Specifically, we analyze the quantum dynamics of a Gaussian wavepacket that exhibits position-momentum correlations. By tuning the parameters governing its evolution, we reveal intriguing effects, with a particular focus on squeezing. Notably, during the wavepacket evolution quantum spreading and squeezing processes emerge, giving rise to Gouy phase contributions of $\pi/4$ rad, establishing a clear link between the Gouy phase and a purely quantum phenomenon. Furthermore, the interplay between wavepacket squeezing and one-dimensional spreading leads to a total Gouy phase accumulation of $\pi/2$ rad in an oscillation period. Both squeezing and Gouy phase have individually proven valuable in state engineering and quantum metrology. By demonstrating a direct, controllable relationship between these two fundamental processes, our findings expand the realm of quantum-enhanced technologies, including quantum sensing and precision measurement.

I. INTRODUCTION

The concept of the Gouy phase was first introduced by L. G. Gouy in 1890, and since its initial detection [1, 2], its properties have been extensively studied [3–6]. The Gouy phase has been applied in various fields, such as in the determination of resonant frequencies within laser cavities [7], phase-matching for strong-field interactions and high-order harmonic generation [8–10], and in the analysis the spatial characteristics of high-repetition-rate laser pulses [11]. This phase is also related to the peculiar characteristic of nondiffracting beams [12], and such beams are a key ingredient for applications ranging from remote sensing [13] to biomedical imaging [14]. For its role in converting light into vortex beams [15–18], the Gouy phase is a crucial parameter in state engineering with applications in communication and optical tweezing [19, 20]. In particular, for quantum information protocols, the entanglement provided by correlated photon-pair sources is fundamental, and the Gouy phase has also been investigated in this context [21]. Recently, the quantum Gouy phase has been measured and confirmed to modify the celebrated photonic de Broglie wavelength, expanding the horizon of quantum-enhanced technology for sensitive measurements [22, 23].

For a particle in a harmonic potential, squeezing leads to a redistribution of uncertainty between position and momentum, thereby creating a correlated state. By enabling state engineering, it modifies the width of the wavepacket, which in turn influences the Gouy phase, offering significant benefits for precision sensing and measurement applications. Furthermore, the Gouy phase of photons in squeezed vacuum states has been linked to the notion of topological phases, indicating a geometric component tied to the structure of the state space [24]. Nonlocal effects of this phase have also been documented [25], where it changes the symmetries connected with self-organization in atomic systems. In the photonic domain, striking a suitable balance between the Gouy phase and the cavity frequency is essential to maintain squeezing in the presence of spatial mode mismatches [26]. Consequently, by manipulating the geometry of beam propagation or the parameters governing squeezing, one can precisely control the quantum phases. This capability is crucial for advancing quantum metrology, interferometry, and quantum information processing.

In multi-transverse-mode systems, squeezing can be applied to enhance the signal-to-noise ratio for specific modes, improving the fidelity of quantum communication. The Gouy phase of vortex light varies in different transverse modes; it can be used to ensure that the squeezing is applied uniformly across all modes [27]. In the context of quantum key distribution (QKD), vortex beams have emerged as a promising platform due to their high-capacity encoding of information—a feature that simultaneously presents considerable challenges for practical deployment. The Gouy phase plays a critical role in addressing these challenges, as it enables the real-time monitoring and correction of wavefront perturbations arising from atmospheric propagation, thereby improving the stability and reliability of

* crislane.brito@umk.pl

† irismarpaz@ufpi.edu.br

QKD protocols. Furthermore, the intrinsic squeezing of the system has been shown to serve as a valuable resource for mitigating quantum noise and decoherence [28].

Squeezed states of massive particles embody a key element for ground-based gravitational wave detectors, gravity-induced entanglement, quantum radars, among others [29]. For instance, cavity-enhanced high-order generated sources are advancing, enabling more accurate measurements and observations at extremely short timescales. Among its potential applications are precise frequency-comb spectroscopy of both electronic and nuclear transitions and low-space-charge attosecond-temporal-resolution photoelectron spectroscopy [30]. Effective phase matching is crucial for such sources to operate efficiently and coherently. Conveniently, optimal power enhancement is achieved by the Gouy phase adjustment [31], where it plays a role in fine-tuning the offset frequency for attosecond pulse generation.

The relevance of the Gouy phase in coherent matter waves was first demonstrated in [32–34] inspiring the subsequent experiments conducted in various systems, including Bose-Einstein condensates [35–37] and astigmatic electron waves [38]. We can also cite its rotation effect observed in electron vortex beams in different situations [17, 18, 39]. We have studied this phase in the context of relativistic matter waves [40, 41] and its nonlocal effects [42]. Digging it further, we found that the Gouy phase for relativistic matter waves contributes to the conversion of orbital angular momentum into spin angular momentum and vice versa [41]. Additionally, in the context of position-momentum correlations, have determined the Gouy phase of SPDC entangled photons [43] and established its connection to measurements of the photons’ quantum correlations. [44]. Recently, we examined the influence of the Gouy phase on an interferometric phenomenon using the Cross-Wigner formalism [45].

In this work, we investigate the quantum dynamics of a massive particle described by a position-momentum correlated Gaussian wavepacket in a harmonic potential. We unravel unique characteristics of matter waves in this setting; by examining various frequency relations and correlation parameter, distinct regimes of squeezing and spreading are uncovered. We notice that the Gouy phase is directly influenced by the squeezing or expansion of the wavepacket, confirming the relation between this phase and the wavepacket width. Notably, although the Gouy phase is usually attributed to transverse confinement, the reversal of its concavity under our conditions indicates that it primarily stems from matter-wave squeezing. In addition, unlike free evolution in one dimension, where the total accumulated Gouy phase is $\pi/4$ rad [32], the inclusion of squeezing effects leads to a total accumulation of $\pi/2$ rad over one oscillation period. We also investigate how one should tune the correlation and the frequency relation to obtain the effects of squeezing or spreading. Squeezing is a valuable quantum resource, as it reduces noise in measurement below the standard quantum limit. Therefore, tailoring the Gouy phase of matter waves to control squeezing represents a powerful tool for quantum sensing and metrology.

The structure of the work is as follows. In Sec. II, we begin by considering that the particle is described by the Gaussian wavepacket of initial width $\sigma_0 = \sqrt{\hbar/(m\omega_0)}$. We assume that the initial state is position-momentum correlated. Then, this initial wavepacket evolves under the propagator of the harmonic oscillator with frequency ω . Owing to the quadratic nature of the dynamics in both position and momentum, the wavepacket remains Gaussian throughout its evolution. We present the analytical expressions for the parameters characterizing the evolved wavepacket, such as the Gouy phase and width, and find that their temporal behaviors are closely connected. In Sec. II A we study the frequency and position-momentum correlation effects on the Gouy phase and wavepacket behavior for a fixed value of time. We investigate the regimes where the current frequency is much smaller ($\omega \ll \omega_0$) and much larger ($\omega \gg \omega_0$) than the fundamental frequency, respectively, in Secs. II B and Sec. II C. We study the dynamics of the Gouy phase and wavepacket in the resonance, in Sec. II D, by considering $\omega = \omega_0$. Notably, when the position-momentum correlation parameter is zero, the wavepacket width remains constant in time, $B(t, \gamma = 0) = \sigma_0$. Under these conditions, there is neither diffraction nor squeezing, causing the phase to vary linearly with time and to lose the characteristic arctan dependence associated with Gaussian wavepackets. We further investigate the limit $|\gamma| \ll 1$, in which the wavepacket width exhibits small oscillations around σ_0 , undergoing minimal spreading and squeezing. Interestingly, the resulting time-dependent phase deviates slightly from the linear profile but preserves the arctan-like Gouy phase signature. Section III summarizes our findings and presents final remarks.

II. HARMONIC EVOLUTION OF A CORRELATED GAUSSIAN WAVEPACKET

It is well known that any mass subjected to a force near a stable equilibrium can, in the leading-order approximation, be modeled as a harmonic oscillator for small vibrations. In other words, most potentials can be approximated by a parabolic potential in the vicinity of a local minimum [46]. Because these phenomena are pervasive in nature, the harmonic oscillator model remains a fundamental cornerstone of modern physics. The harmonic approximation is applicable across a broad array of physical systems, with ion traps serving as a notable example, since they offer a robust platform for quantum mechanical investigations owing to the extended coherence times of both internal and motional states [47]. In the context of cavity-QED experiments, the relevance of the harmonic oscillator is to describe the electromagnetic field mode inside the cavity, whereas in the ion case, its relevance is associated with describing the

ion's motion [47]. The applications range from quantum simulations [48] to quantum sensing [49, 50] and quantum information processing [51, 52].

In describing confined matter waves, we examine the evolution of a position-momentum correlated Gaussian wavepacket for a massive particle in a harmonic potential. Although the wavepacket retains its Gaussian form throughout the evolution, its defining parameters—including the Gouy phase and wavepacket width—differ significantly from those associated with free evolution [32].

We begin by considering the initial state described by the correlated Gaussian wavefunction of transverse width $\sigma_0 = \sqrt{\hbar/(m\omega_0)}$

$$\psi_0(x') = \frac{1}{\sqrt{\sigma_0}\sqrt{\pi}} \exp\left[-\frac{x'^2}{2\sigma_0^2} + \frac{i\gamma x'^2}{2\sigma_0^2}\right], \quad (1)$$

where ω_0 is the intrinsic spread frequency of the initial wavepacket. This state represents an approximately localized state in another potential, which does not necessarily correspond to an eigenstate of the harmonic oscillator within which we will consider the particle to be confined. The initial position-momentum correlation will be represented by the real correlation parameter γ , which can take values in the interval $-\infty < \gamma < \infty$. It is worth mentioning that the position-momentum correlation is related to the complex squeezing parameter, which produces squeezing plus rotation effects [53, 54]. This parameter is related to the Pearson product-moment (PM) correlation coefficient r which satisfies $-1 \leq r \leq 1$. The position-momentum correlation has been shown to be linked to the Gouy phase [32], as well as to the number of interference fringes, squeezing, and quantum coherence effects in the context of the double-slit experiment [55, 56]. Additionally, it has been connected to time interference explored through the Cross-Wigner formalism [45]. We can also mention its effect on coherence freezing [57] and its role in enhancing Gaussian quantum metrology [58]. Here, it influences the confined dynamics, leading to distinct modifications in the wavepacket evolution.

The temporal evolution of the position-momentum correlated wavepacket within a harmonic potential is obtained as follows

$$\psi(x, t) = \int_{-\infty}^{\infty} dx' G(x, t; x', 0) \psi_0(x'), \quad (2)$$

where

$$G(x, t; x', 0) = \sqrt{\frac{m\omega}{2\pi i\hbar \sin \omega t}} e^{\left[\frac{im\omega}{2\hbar \sin \omega t} [\cos \omega t (x^2 + x'^2) - 2xx']\right]}. \quad (3)$$

The kernel $G(x, t; x', 0)$ is the nonrelativistic propagator of the harmonic oscillator for a particle of mass m subject to a harmonic potential of frequency ω [59]. Throughout the text, we refer to this frequency as the natural frequency of the confining harmonic oscillator. Finally, $\psi_0(x')$ is the initial wavepacket Eq. (1).

After some algebraic manipulations in the expression obtained from Eq. (2), we can write the temporal state of a massive particle with spatial-momentum correlations in a harmonic potential as

$$\psi(x, t) = \frac{1}{\sqrt{B}\sqrt{\pi}} \exp\left(-\frac{x^2}{2B^2}\right) \exp\left(\frac{imx^2}{2\hbar R} - i\mu\right), \quad (4)$$

where

$$B^2(t, \gamma) = \sigma_0^2 \left(\frac{\omega_0}{\omega}\right)^2 \left\{ \sin^2 \omega t + [\gamma \sin \omega t + (\omega/\omega_0) \cos \omega t]^2 \right\}, \quad (5)$$

$$R(t, \gamma) = \frac{C(t) \sin \omega t}{\omega C(t) \cos \omega t - (\omega^2/\omega_0) [\gamma \sin \omega t + (\omega/\omega_0) \cos \omega t]}; \quad (6)$$

$$C(t) = \sin^2 \omega t + [\gamma \sin \omega t + (\omega/\omega_0) \cos \omega t]^2,$$

and

$$\mu(t, \gamma) = \frac{1}{2} \arctan \left[\frac{\sin \omega t}{\gamma \sin \omega t + (\omega/\omega_0) \cos \omega t} \right]. \quad (7)$$

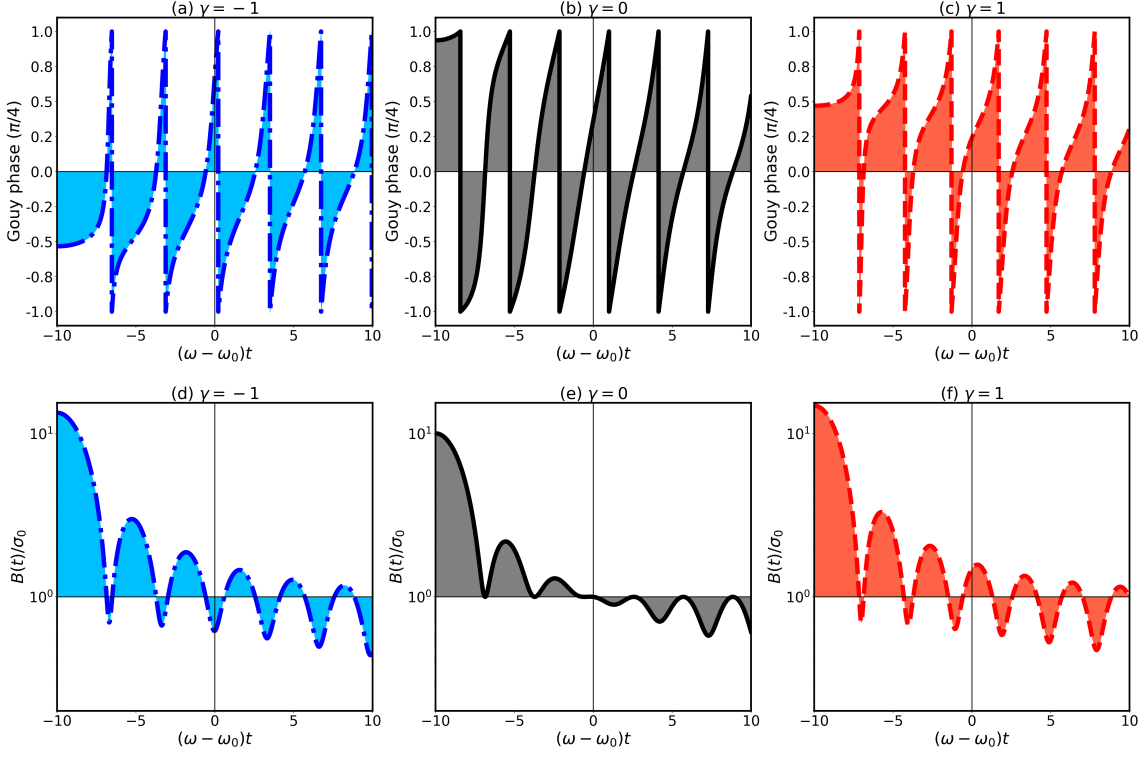


FIG. 1. Gouy phase and wavepacket width as a function of the natural frequency of the confining oscillator ω , for the intrinsic frequency of the particle $\omega_0 = 10$ Hz and time evolution $t = 1$ s. For ease, we choose generic values of frequencies, however, the behavior remains as far as the relation between the mismatch frequencies in a real experimental is the same as proposed here. Three values of position-momentum correlations γ are considered, with $\gamma = -1$ in (a) and (d) (blue dash-dot), $\gamma = 0$ in (b) and (e) (black solid line), and $\gamma = 1$ in (c) and (f) (red dashed). The wavepacket width oscillates as a function of $\omega - \omega_0$ (bottom plots), presenting regions of squeezing and spread. For $\omega < \omega_0$ and $|\gamma| \neq 0$, we observe squeezing and spreading in each period but the spread is more evident. For $\omega > \omega_0$ and $|\gamma| \neq 0$, the squeezing is more evident and grows stronger far from the resonance limit where $\omega \gg \omega_0$. For the position-momentum correlation $\gamma = 0$ the wavepacket only spreads for $\omega < \omega_0$ and only squeezes for $\omega > \omega_0$. The squeezing effect is crucial for the Gouy phase accumulation (top plots), which is completely different for the free evolution case, where the Gouy phase is accumulated when the wavepacket spread from the initial width and the total Gouy phase accumulated is only $\pi/4$ rad. Here, squeezing and spreading effects contribute to the total acquired Gouy phase of $\pi/2$ rad.

Here, $B(t, \gamma)$ is the wavepacket width, $R(t, \gamma)$ is the wavefront curvature radius, and $\mu(t, \gamma)$ is the Gouy phase for the propagation through the harmonic potential. We can also identify $\tau_0 = \omega_0^{-1}$ as the time scale (“the Rayleigh time”) that governs the spread of the wavepacket in the free evolution and has the same role of the Rayleigh length in the propagation of paraxial light waves [32].

Similarly to the free evolution, the rate of temporal variation of the Gouy phase is directly related to the wavepacket width by

$$\frac{\partial \mu(t, \gamma)}{\partial t} = \frac{\omega_0}{2[B(t, \gamma)/\sigma_0]^2}, \quad (8)$$

which can be easily obtained by deriving Eq. (7) with respect to time. As can be seen from Eq. (8), the Gouy phase shift rate can be associated with the wavepacket spatial confinement [60], with the constant rate characterizing the nondiffracting wavepacket as a direct consequence of its profile spatial invariance [12]. From Eq. (8), one obtains that $\frac{\partial^2}{\partial t^2} \mu(t, \gamma) \propto \frac{\partial}{\partial t} B(t, \gamma)$, which produces $\frac{\partial^2}{\partial t^2} \mu(t, \gamma) = 0$ for the values of time at which the wavepacket width is either maximum or minimum. Therefore, in this condition, the Gouy phase will change its concavity and/or sign.

A. Oscillator Frequency and Correlation Effects

Here, we analyze the relation between the Gouy phase and the wavepacket width by fixing the propagation time and the initial wavepacket frequency, while varying the natural frequency of the oscillator and the initial position-momentum correlations. Note that the initial frequency of the particle differs from the natural frequency of the harmonic oscillator in which it is confined. As a result, the system is not initially in an eigenstate, leading to an adjustment of the wavepacket shape. In Fig. 1, we plot the Gouy phase and the wavepacket width as a function of the frequency mismatch ($\omega - \omega_0$), for different values of the position-momentum correlation parameter γ .

We fix the characteristic frequency of the particle at $\omega_0 = 10$ Hz, the propagation time at $t = 1$ s, and consider three different values of the correlation parameter:

- $\gamma = -1$ (blue dash-dot) in Fig. 1(a) and Fig. 1(d),
- $\gamma = 0$ (black solid) in Fig. 1(b) and Fig. 1(e),
- $\gamma = 1$ (red dashed) in Fig. 1(c) and Fig. 1(f).

For clarity, the Gouy phase (top plots) is expressed in units of $\pi/4$ rad, while the wavepacket width $B(t, \gamma)$ (bottom plots) is given in units of σ_0 (the initial wavepacket width).

As expected from Eq. (8), the Gouy phase changes its concavity at the time values where the wavepacket width reaches its maximum. Notably, for $\gamma < 0$, the concavity change occurs in the negative portion of the Gouy phase, whereas for $\gamma > 0$, the transition appears in its positive portion. This behavior encodes a distinct signature in the Gouy phase, reflecting the change in squeezing rotation direction caused by the sign reversal of the correlation parameter. For $\gamma = 0$, the concavity transition occurs precisely when the Gouy phase is zero.

The wavepacket width oscillates as a function of $\omega - \omega_0$ (bottom plots), presenting regions of squeezing and spread. For $\omega < \omega_0$ and $|\gamma| \neq 0$, we observe squeezing and spreading in each period, but the spreading is more evident and becomes even stronger far from the resonance regime, where the oscillator's eigenfrequency is much smaller than the particle's intrinsic frequency $\omega \ll \omega_0$. On the other hand, for $\omega > \omega_0$ and $|\gamma| \neq 0$, the squeezing is more evident and grows stronger far from the resonance limit, where the natural frequency of the oscillator is much larger than the frequency of the initial wavepacket $\omega \gg \omega_0$. Interestingly, for the position-momentum correlation $\gamma = 0$ the wavepacket only spreads for $\omega < \omega_0$ and only squeezes for $\omega > \omega_0$, with the intensity of these effects always smaller than for the cases where $\gamma \neq 0$. Such effects are further enhanced when larger values of $|\gamma|$ are considered, i.e., the role of the position-momentum correlations is to produce squeezing and spreading in both intervals of the frequency difference. It is worth mentioning that squeezing means that the wavepacket width becomes smaller than σ_0 , the width of the initial Gaussian state. This is equivalent to say that the uncertainty in position becomes smaller than that of the vacuum state of the harmonic oscillator while the other quadrature expands.

For matter waves undergoing free evolution, the Gouy phase begins to accumulate as wavepacket spreads from its initial width, reaching a total accumulation of $\pi/4$ rad [32]. In contrast, we notice that for matter waves confined within a one-dimensional harmonic potential, the total Gouy phase acquired is $\pi/2$. Interestingly, the squeezing effect-determined by the frequency difference $\omega - \omega_0$ and position-momentum correlation γ -plays a crucial role in the Gouy phase accumulation (as shown in the top plots), connecting the Gouy phase with a purely quantum feature. Therefore, both squeezing and spreading effects contribute to the total Gouy phase of $\pi/2$ rad. Note that a total Gouy phase of $\pi/2$ can be acquired in regions without squeezing, as illustrated on the left side of Fig. 1(b) and (e), we have an analogous of the focusing effect where half of the phase accumulates as the wavepacket at a maximum width converges to the initial width, while the other half is gained as it expands back to its maximum width. A summary of the frequency and correlation regimes and their consequences on the wavepacket width and Gouy phase is presented in Table I.

In the next subsections, we will analyze the behaviors of the Gouy phase and wavepacket width for different regimes of the harmonic oscillator's natural frequency by varying the propagation time and the initial position-momentum correlations.

TABLE I. Summary of wavepacket width and Gouy phase behavior as a function of frequency mismatch $\omega - \omega_0$ and position-momentum correlation γ .

Frequency Regime	γ Condition	Wavepacket Width Behavior	Gouy Phase Accumulation
$\omega < \omega_0$	$ \gamma \neq 0$	Oscillates with both squeezing and spreading; spreading dominates, especially when $\omega \ll \omega_0$.	Total Gouy phase of $\pi/2$ rad (squeezing contribution).
$\omega > \omega_0$	$ \gamma \neq 0$	Oscillates with both squeezing and spreading; squeezing dominates, especially when $\omega \gg \omega_0$.	Total Gouy phase of $\pi/2$ rad (squeezing contribution).
$\omega > \omega_0$	$\gamma = 0$	Only squeezing is observed; effects are less intense than for $ \gamma \neq 0$.	Total Gouy phase of $\pi/2$ rad (squeezing contribution).
$\omega < \omega_0$	$\gamma = 0$	Focusing effect; Spreading and contraction are observed; effects are less intense than for $ \gamma \neq 0$.	Total Gouy phase of $\pi/2$ rad (no squeezing contribution).

B. Time and Correlation Effects for $\omega \ll \omega_0$

The Gouy phase and wavepacket features are further investigated here as a function of time in the far-from-resonance regime, considering the case where the natural frequency of the harmonic oscillator is much smaller than the intrinsic frequency of the particle, i.e., $\omega \ll \omega_0$.

The behavior of the Gouy phase is directly linked to the wavepacket width, as indicated by Eq. (8). We confirm the validity of this relation over time by examining Fig. 2, where the Gouy phase (in units of $\pi/4$ rad) and the wavepacket width (in units of σ_0) are plotted against time in the regime $\omega \ll \omega_0$. We consider a natural frequency of the oscillator, $\omega = 0.1$ Hz, an intrinsic frequency associated with the initial wavepacket of the particle, $\omega_0 = 1$ Hz, and three different values of the correlation parameter γ . In Fig. 2(a), we show the Gouy phase, and in Fig. 2(b), the wavepacket width at shorter timescales. In Fig. 2(c) and Fig. 2(d), we extend the evolution to longer times and display both the Gouy phase and the wavepacket width on the same plot for $\gamma = 0$ and $\gamma = 1$, respectively. In Fig. 2(c) and Fig. 2(d), the Gouy phase is represented in black, associated with the left axis, while the wavepacket width is plotted in red, aligned with the right axis.

As observed, for short times, the free-dynamics behavior is recovered, with the Gouy phase evolving to its maximum value of $\pi/4$ rad. Within this time range, for both $\gamma = 0$ and $\gamma = 1$, the wavepacket spreads. This spreading occurs more rapidly for $\gamma = 1$, causing a delayed evolution of the Gouy phase towards $\pi/4$ rad relative to $\gamma = 0$. For position-momentum anticorrelation $\gamma = -1$, the wavepacket initially contracts to a minimum width before expanding. Both effects contribute to the Gouy phase, which rises quickly to the maximum value of $\pi/4$ rad for $\gamma = -1$. The behavior for short times can be observed in the approximate formulas A1 (wavepacket width) and A2 (Gouy phase) in Appendix A. In fact, the first terms of each expression correspond to the free-dynamics expressions [56].

Meanwhile, for longer propagation times, the wavepacket width exhibits local maxima and minima points. As indicated by Eq. (8), the time instants corresponding to the local extrema of the wavepacket width are related to changes in concavity and sign of the associated Gouy phase. For instance, for $\gamma = 0$, as shown in Fig. 2(c), the time at which the wavepacket width reaches its maximum corresponds to the instant at which the Gouy phase exhibits a discontinuous sign change, while the time at which the wavepacket width reaches its minimum corresponds to an instant when the Gouy phase undergoes a continuous transition in both sign and concavity.

Note that for $\gamma = 0$, within the examined frequency range, the wavepacket remains unsqueezed, so that $B(t, \gamma = 0) \geq \sigma_0$. Another interesting characteristic is observed when the wavepacket evolves from its maximum width at around $t = 15.7$ s to the next maximum at around $t = 47.1$ s; we observe a one-dimensional focusing effect. In this interval, the wavepacket converges to the minimum value σ_0 and then expands thereafter. Within the time interval where the focusing effect is observed, the total Gouy phase accumulated is $\pi/2$ rad.

For $\gamma = 1$, Fig. 2(d), the maxima and minima values of the wavepacket width remain at the same values of time for $\gamma = 0$, i.e., the value of γ does not contribute to the time of maxima and minima of the wavepacket width. In contrast to the case $\gamma = 0$, the times corresponding to the maxima of the wavepacket width are associated with changes in the concavity of the Gouy phase, while the times corresponding to the minima are linked to discontinuous changes in the sign of the Gouy phase. Here, we can also observe squeezing of the wavepacket and this effect is crucial for the total accumulation of $\pi/2$ rad for the Gouy phase. Observe that around $t = 0$ we do not have squeezing and the total Gouy phase accumulated from $t = 0$ to $t = 31.4$ s is only $\pi/4$ rad. In contrast, the evolution from $t = 31.4$ s to 62.8 s accumulates a total Gouy phase of $\pi/2$ rad because we have squeezing around $t = 31.4$ s as well as around $t = 62.8$ s. We do not present the case $\gamma = -1$ for longer time values, as it would result in a qualitatively analogous

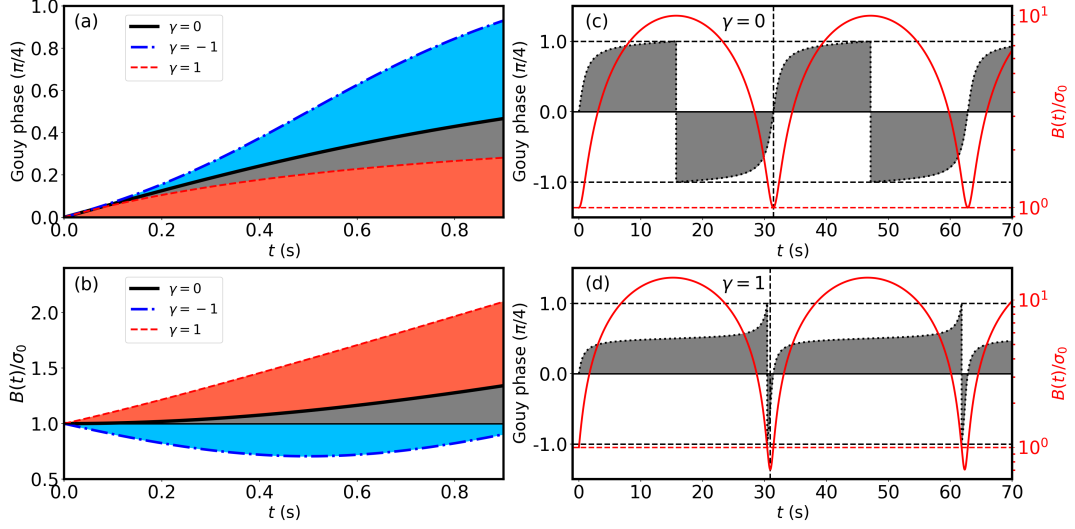


FIG. 2. Temporal behavior of the Gouy phase and wavepacket width for low harmonic oscillator's frequency $\omega \ll \omega_0$. We consider $\omega = 0.1 \text{ Hz} \ll \omega_0 = 1 \text{ Hz}$ and three values of the correlation parameter γ . (a) Gouy phase and (b) wavepacket width for small values of the propagation time. In (c) and (d) Gouy phase and wavepacket width at the same plot for $\gamma = 0$ and $\gamma = 1$, respectively. Here, large values of propagation time are considered. In (c) and (d) the Gouy phase corresponds to the left scale and the black color while the wavepacket width corresponds to the right scale and the red color. The free dynamics are recovered for smaller values of time where the Gouy phase evolves to the maximum value of $\pi/4$ rad. Within this range of time and for $\gamma = 0$ and $\gamma = 1$, the wavepacket only spreads, which implies a slow evolution of the corresponding Gouy phase to its maximum value $\pi/4$ rad. For position-momentum anti-correlation $\gamma = -1$, the wavepacket first squeezes from the initial width to a minimum width and then spreads from it. Both effects contribute to the Gouy phase, which evolves rapidly to the maximum value $\pi/4$ rad for $\gamma = -1$. For larger values of propagation time, the wavepacket width presents local maxima and minima values. These values of times for the maxima and minima wavepacket width are related with changes in the concavity and/or sign of the corresponding Gouy phase. For $\gamma = 0$, within the range of frequencies considered here, the wavepacket never squeezes. We see an effect similar to focusing (lens effect) on one dimension when the wavepacket propagates from its maximum width at around $t = 15.7 \text{ s}$ to the next maximum at around $t = 47.1 \text{ s}$. Within this time interval the total Gouy phase accumulated is $\pi/2$ rad. For $\gamma = 1$ the squeezing of the wavepacket is crucial for the total accumulation of $\pi/2$ rad for the Gouy phase.

case of $\gamma = 1$, which we have already presented. An overview of the results discussed in this section is presented in Table II.

TABLE II. Summary of wavepacket width $B(t, \gamma)$ and Gouy phase $\mu(t, \gamma)$ for $\omega = 0.1 \text{ Hz} \ll \omega_0 = 1 \text{ Hz}$ and three values of γ . Short-time results (up to $t \approx 1 \text{ s}$) match panels (a) and (b) of Fig. 2; long-time results (up to $t = 70 \text{ s}$) correspond to panels (c) and (d).

(γ, time)	$B(t)/\sigma_0$	$\mu(t)$
$\gamma = -1$, short	Rapid initial squeezing	Quick rise toward $\pi/4$
$\gamma = -1$, long	Oscillates with large spread and small squeezing	Accumulates $\pi/2$ in each period
$\gamma = 0$, short	Spreading	Gradual increase from 0 to $\pi/4$
$\gamma = 0$, long	Instead of squeezing there is focusing effect	Accumulates $\pi/2$
$\gamma = 1$, short	Rapid initial spreading	Slower growth
$\gamma = 1$, long	Oscillates with large spread and small squeezing	Accumulate $\pi/2$ in each period

C. Time and Correlation Effects for $\omega \gg \omega_0$

We focus once more on the off-resonance dynamics, but now we consider the opposite end of the frequency spectrum. We examine the temporal evolution of the wavepacket in the regime where the natural frequency of the oscillator is much larger than the intrinsic frequency of the particle, i.e., $\omega \gg \omega_0$, as well as the effects of the initial position-

momentum correlation.

The Gouy phase (in units of $\pi/4$ rad) and the wavepacket width (in units of σ_0) as a function of time in this regime are presented in Fig. 3. We consider $\omega = 10$ Hz, $\omega_0 = 1$ Hz and three different values of the correlation parameter γ . In Fig. 3(a) and Fig. 3(b) we consider $\gamma = 0$ and $\gamma = -10$. In Fig. 3(c) and Fig. 3(d) we consider $\gamma = 0$ and $\gamma = 10$.

The width of the wavepacket oscillates in time, and a total Gouy phase shift of $\pi/2$ rad is accumulated between successive minima of the wavepacket width. Unlike the behavior observed in the regime where the oscillator's eigenfrequency is lower than the intrinsic frequency of the particle, the width of the wavepacket remains squeezed for $\gamma = 0$, with its width always smaller than or equal to the initial width. For $\gamma = 10$ and $\gamma = -10$ the wavepacket undergoes squeezing, although there exist time intervals where its width exceeds the initial value. Here, the changes produced by $|\gamma| = 1$ is very small, therefore we consider large values of $|\gamma|$ in order to see the initial position-momentum correlations effect in this frequency regime. For $\gamma = 0$, the time at which the wavepacket reaches its maximum width coincides with the time at which the Gouy phase undergoes changes in both concavity and sign. Moreover, for $\gamma \neq 0$ the time when the wavepacket is maximum corresponds to the instant when the Gouy phase concavity changes.

Interestingly, the total Gouy phase of $\pi/2$ rad is acquired in each period for any value of γ when the wavepacket evolves from a point of maximum squeezing (minimum width) until the next point of maximum squeezing. This way of accumulating the Gouy phase is different from the usual focusing process, where a light or matter-wave beam first converges to the focus and then spreads out [33]. Moreover, the rapid accumulation of the Gouy phase is advantageous for quantum metrology applications [23].

The approximated expressions for the wavepacket width and Gouy phase in the regime discussed above are given, respectively, in Eq. (A3) and Eq. (A4) of Appendix A. We summarize the key behaviors of the wavepacket width and the Gouy phase under different correlation effects in the $\omega \gg \omega_0$ regime in Table III.

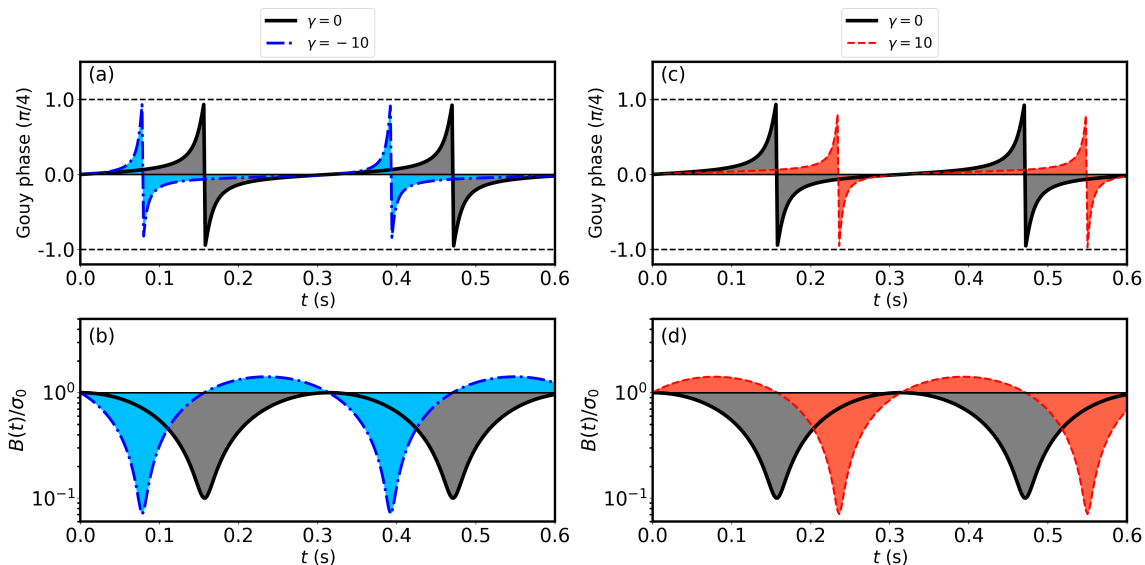


FIG. 3. Temporal behavior of the Gouy phase and wavepacket width when the oscillator's frequency is much larger than the intrinsic frequency of the particle $\omega \gg \omega_0$. We consider $\omega = 10$ Hz and $\omega_0 = 1$ Hz. Panels (a) and (b) compare the dynamics for $\gamma = -10$ with respect to $\gamma = 0$, while panels (c) and (d) illustrate the case of $\gamma = 10$ versus $\gamma = 0$. The width of the wavepacket exhibits temporal oscillations, with a total Gouy phase shift of $\pi/2$ rad accumulated during the interval of time between two successive minima of the wavepacket width. The wavepacket width is always squeezed for $\gamma = 0$. For $\gamma = 10$ and $\gamma = -10$ the wavepacket squeezes and spread above its initial width.

TABLE III. Key behaviors in the off-resonance regime ($\omega \gg \omega_0$).

Off-Resonance Regime: $\omega \gg \omega_0$			
γ	Gouy Phase	Wavepacket Width	Correlation Effects
0	$\pi/2$ per cycle	Remains squeezed	Minimum width reached at regular intervals
+10	$\pi/2$ per cycle	Strong oscillations; width exceeds a little the initial value	Minimum width reached later than for $\gamma = 0$
-10	$\pi/2$ per cycle	Strong oscillations; width exceeds a little the initial value	Minimum width reached earlier than for $\gamma = 0$

D. Time and Correlation Effects in the Resonance $\omega = \omega_0$

In this section, we study the dynamics of the Gouy phase and wavepacket width in the resonant regime, where the initial frequency of the particle matches the natural frequency of the confining harmonic oscillator. In this scenario, the results are strongly influenced by the position-momentum correlation parameter γ . It comes from the fact that, if there is no position-momentum correlation, the initial Gaussian wavepacket is an eigenstate of the harmonic oscillator and would acquire only a global phase. Notably, by varying γ , one can observe characteristics of a slowly diffracting wavepacket. Then, we consider $\omega = \omega_0$, which produces for the wavepacket width and the Gouy phase, respectively, the following results

$$B^2(t, \gamma) = \sigma_0^2 \left[\sin^2 \omega t + (\gamma \sin \omega t + \cos \omega t)^2 \right], \quad (9)$$

and

$$\mu(t, \gamma) = \frac{1}{2} \arctan \left(\frac{\sin \omega t}{\gamma \sin \omega t + \cos \omega t} \right). \quad (10)$$

Note that for an initially uncorrelated Gaussian state $\gamma = 0$, the wavepacket width is time independent, i.e., $B(t, \gamma = 0) = \sigma_0$, and the Gouy phase is linear with the propagation time, i.e., $\mu(t, \gamma = 0) = \frac{\omega t}{2}$, in agreement with the Gouy phase of a Bessel beam [61]. Therefore, in resonance ($\omega = \omega_0$) and for $\gamma = 0$, the wavepacket is nondiffracting and its Gouy phase does not follow the conventional arctan profile characteristic of diffracting Gaussian wavepackets.

In Fig. 4, we show the Gouy phase (in units of $\pi/4$ rad) and the wavepacket width (in units of σ_0) in the resonant regime, as a function of propagation time t , for three distinct values of the initial correlation γ . Fig. 4(a) and Fig. 4(c) correspond to $\gamma = -1$, and Fig. 4(b) and Fig. 4(d) to $\gamma = 1$. It can be observed that as the frequency increases, the period of the Gouy phase decreases, i.e., the total Gouy phase of $\pi/2$ rad can be acquired in a small interval of time. Moreover, it is important to highlight that the period, given by π/ω , remains independent of the initial correlation parameter γ , but it is affected by a time shift due to changes in the squeezing direction. Different from the regimes explored above, respectively, $\omega \ll \omega_0$ and $\omega \gg \omega_0$, in the resonant regime, although the spreading is more pronounced, the difference between spreading and squeezing is less extreme.

Again, the total Gouy phase of $\pi/2$ acquired in each period is a consequence of spreading and squeezing. The maxima values of the wavepacket width give the values of time for which the Gouy phase changes its concavity. Inside each period, the total Gouy phase is acquired in two parts of the time evolution.

- For $\gamma = -1$, the Gouy phase of $\pi/4$ rad is accumulated when the wavepacket evolves from a point of maximum squeezing (minimum width) until the second value of time for which the wavepacket width becomes equal to the width of the initial wavepacket. Another portion of $\pi/4$ rad is acquired when the wavepacket squeezes until the next point of maximum squeezing.
- For $\gamma = 1$, $\pi/4$ rad is obtained when the wavepacket evolves from a point of maximum squeezing until the first value of time for which the wavepacket width becomes equal to the initial width. The last portion of $\pi/4$ rad is accumulated when the wavepacket evolves from this point to the next point of maximum squeezing.

The difference in the results of the Gouy phase produced by $\gamma = -1$ and $\gamma = 1$ happens because the direction of squeezing is changed such that for $\gamma = -1$ the wavepacket starts the evolution squeezing and for $\gamma = 1$ it starts spreading.

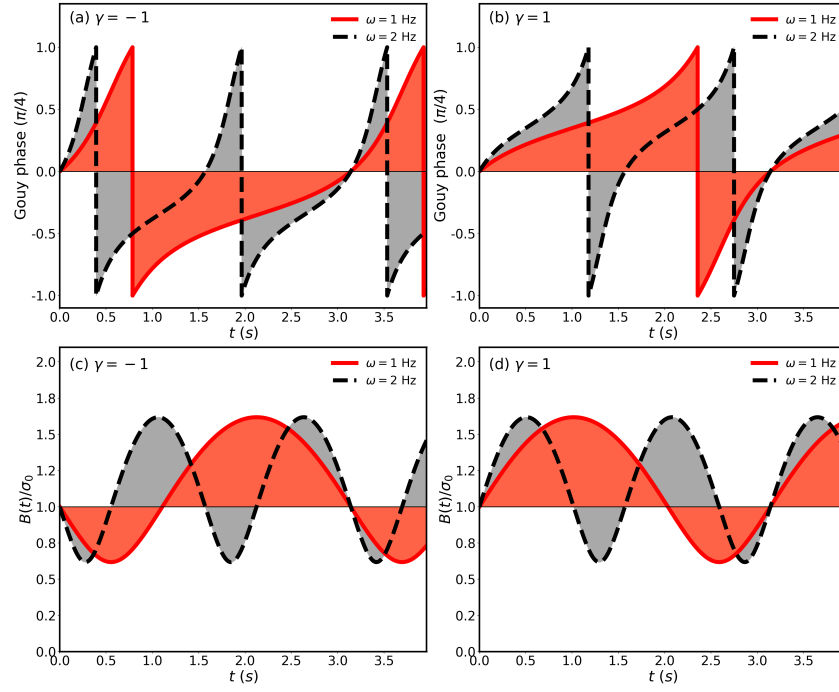


FIG. 4. Gouy phase and wavepacket width in the resonance as a function of propagation time t , for three distinct values of the initial correlation γ . Panels (a) and (c) correspond to $\gamma = -1$, and panels (b) and (d) to $\gamma = 1$. It can be observed that as the frequency increases, the period of the Gouy phase decreases. Additionally, it is noteworthy that the period, given by π/ω , remains independent of the initial correlation parameter γ , but it is affected as a time translation because of the changing in the squeezing direction. In the resonance the wavepacket spreads and squeezes, with spreading effect being more intense. The total Gouy phase of $\pi/2$ acquired in each period is a consequence of spreading and squeezing.

Next, to better understand the effects of time evolution and the initial position-momentum correlations on the acquired Gouy phase, we exhibit the contour plots of this phase in Fig. 5. In Fig. 5(a), we present the Gouy phase, while in Fig. 5(b), we display the contour plot of the wavepacket width as functions of the correlation parameter γ and the propagation time t , for $\omega = \omega_0 = 1$ Hz. As before, the Gouy phase is expressed in units of $\pi/4$ rad and the wavepacket width in units of σ_0 . We can observe by the color mapping that there are regions of squeezing of the wavepacket where $B(t, \gamma) < \sigma_0$ (represented in dark blue) and regions of spreading where $B(t, \gamma) > \sigma_0$ (depicted in dark red). The contour plot reveals that while squeezing occurs for both positive and negative γ , the variation profile differs, reflecting the dependence of the squeezing direction on the sign of γ . The Gouy phase accumulates the total quantity of $\pi/2$ rad when the correlation parameter and the propagation time change. The accumulated portion of $-\pi/4$ rad is related to the wavepacket squeezing and the accumulated portion of $\pi/4$ rad to the wavepacket spreading. Also, we can see that squeezing and spreading effects are intensified as $|\gamma|$ increases. Only one period is shown for clarity. A panoramic overview of the correlation effects on the Gouy phase and wavepacket width in the resonance regime is shown in Table IV.

TABLE IV. Key behaviors in the resonant regime ($\omega = \omega_0$). The Gouy phase accumulates $\pi/2$ each period, and nonzero γ shifts the timing and extent of squeezing/spreading.

Resonance Regime: $\omega = \omega_0$			
γ	Gouy Phase	Wavepacket Width	Correlation Effects
-1	$\pi/2$ per period	Initially narrower, then spreads and resqueezes	Negative correlation shifts squeezing earlier
0	Linear profile	No changing	No effect
+1	$\pi/2$ per period	Initially wider, then squeezes and re-expands	Positive correlation delays minimum width

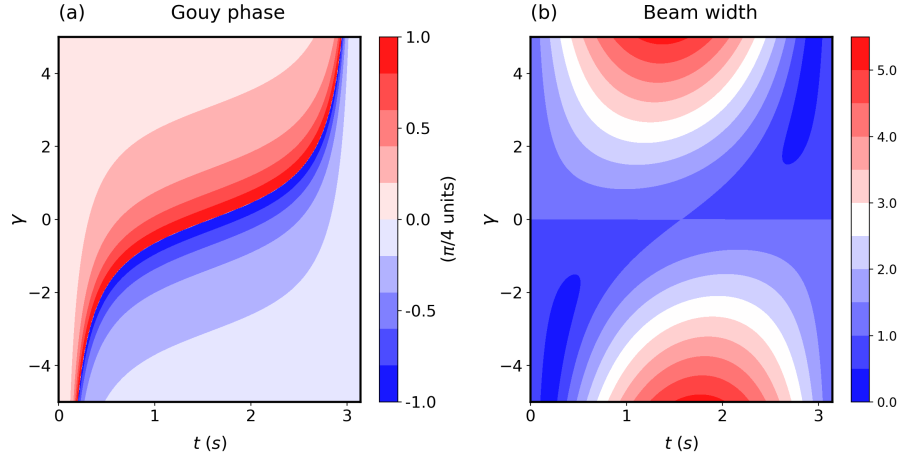


FIG. 5. One period of the (a) Gouy phase and (b) wavepacket width contour plots as a function of correlation parameter γ and the propagation time t for $\omega = \omega_0 = 1$ Hz. Gouy phase is expressed in units of $\pi/4$ rad and the wavepacket width in units of σ_0 . There are regions of squeezing of the wavepacket where $B(t, \gamma) < \sigma_0$ (more visible as dark blue color) and regions of spreading where $B(t, \gamma) > \sigma_0$ (more visible as dark red color). The Gouy phase accumulates the total quantity of $\pi/2$ rad when the correlation parameter and the propagation time change.

E. Slowly varying wavepackets

We explore further into the resonance regime, focusing on scenarios where the wavepacket exhibits only minor temporal variations from its initial state. It still accumulates the total Gouy phase of $\pi/2$ rad, while retaining an approximately linear temporal profile. In fact, as pointed out in [12], a real beam whose Gouy phase is close to that linear evolution in a given range will have nondiffracting properties in such a range. Here, the initial position-momentum correlation represented by the parameter γ governs such behavior. In other words, the departure from the linear dependence on t of the Gouy phase will determine the degree of nondiffracting behavior of such a wavepacket. In the context of light waves, the Gouy phase of nondiffracting beams has been studied theoretically and experimentally [61, 62]. Such light beams offer applications in biomedicine, microscopy, manipulation of microscopic particles, particle manipulation, precision measurements, and enhanced image resolution and contrast [13, 14, 63–65]. Thus, given the importance and the vast range of applications of nondiffracting (or almost nondiffracting) beams in the field of light, it is crucial to rigorously determine the propagation regimes and conditions under which a correlated Gaussian matter-wavepacket, with finite energy and spatial extent, exhibits nondiffracting behavior.

The regime of nearly nondiffracting wavepackets can be achieved in the resonance condition ($\omega = \omega_0$) and for $\gamma \ll 1$, where the Gaussian wavepacket width will undergo only slight oscillations about its initial width. In this limit, we obtain the following expressions for the Gouy phase and the wavepacket width

$$\mu(t) \approx \frac{\omega t}{2} - \frac{1}{2} \sin^2(\omega t) \gamma + \mathcal{O}(\gamma^2), \quad (11)$$

and

$$B(t) \approx \sigma_0 + \frac{1}{2} \sigma_0 \sin(2\omega t) \gamma + \mathcal{O}(\gamma^2). \quad (12)$$

We display their behavior as functions of ωt for small values of the correlation parameter γ in Fig. 6. In Fig. 6(a) we show the Gouy phase and in Fig. 6(b) the wavepacket width. The black solid line corresponds to $\gamma = 0$, the blue dash-dot line to $\gamma = 0.1$ and the red dashed line to $\gamma = 0.5$. For $\gamma = 0$ the wavepacket is nondiffracting, and the corresponding Gouy phase increases linearly with time. For small values of γ , the wavepacket width presents small oscillations around the initial width while the phase deviates slightly from the linear profile but preserves the key features of the Gouy phase typical of diffracting Gaussian wavepackets, with a total phase shift of $\pi/2$ rad in each period. For even smaller values of γ , such deviation of the wavepacket width and Gouy phase is further reduced, suggesting that an almost nondiffracting wavepacket can be engineered. This kind of wavepacket can be useful in applications similar to those of nondiffracting light beams, such as nearly nondiffracting neutron or electron beams. Also, such wavepackets can be useful to reduce the effects of decoherence associated with wavepacket spreading [28].

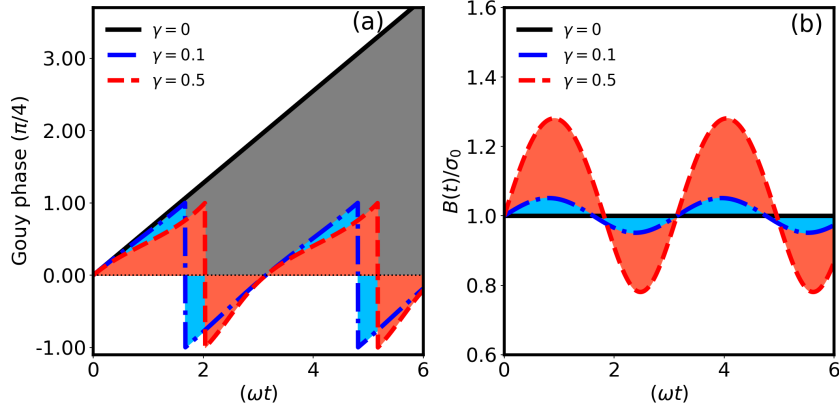


FIG. 6. Gouy phase and wavepacket width as functions of ωt for small values of correlation parameter γ . Panel (a) is the Gouy phase and panel (b) is the wavepacket width. The black solid line corresponds to $\gamma = 0$, the blue dash-dot line to $\gamma = 0.1$ and the red dashed red line to $\gamma = 0.5$.

III. CONCLUSION

We studied the quantum dynamics of a Gaussian wavepacket with position-momentum correlations, characterized by the correlation parameter γ , for a particle of intrinsic frequency ω_0 confined in a harmonic potential with frequency ω , focusing on the behavior of the Gouy phase and wavepacket width. The case $\gamma = 0$ corresponds to the fundamental state of a harmonic oscillator of frequency ω_0 . These three parameters govern the wavepacket dynamics and lead to interesting effects such as squeezing.

We discussed the wavepacket and Gouy phase profiles for different regimes of confinement. In the off-resonance regimes $\omega \ll \omega_0$ and $\omega \gg \omega_0$, we observed that the wavepacket exhibits distinct squeezing and spreading behaviors, which are strongly modulated by the position-momentum correlations. For $\omega \ll \omega_0$, the wavepacket predominantly spreads, with squeezing effects becoming more pronounced for larger values of γ and no squeeze for $\gamma = 0$. Although the squeezing effect is small when the frequency of the harmonic oscillator is much smaller than the intrinsic frequency of the particle, it is still crucial for the acquired Gouy phase. Conversely, in the regime where the oscillator's frequency is much larger than the intrinsic frequency of the particle $\omega \gg \omega_0$, the wavepacket remains squeezed for $\gamma = 0$, while for $\gamma \neq 0$, it alternates between squeezing and spreading. Notably, the Gouy phase accumulation is closely tied to the wavepacket's dynamics, with squeezing and spreading effects playing complementary roles in its evolution. These behaviors directly influence the accumulation of the Gouy phase, which reaches a total of $\pi/2$ rad over specific intervals of propagation time. In the resonant regime $\omega = \omega_0$, the system exhibits unique characteristics, particularly for small values of γ . Here, the wavepacket width remains nearly constant, and the Gouy phase evolves linearly with time, mimicking the behavior of nondiffracting beams. For $\gamma \ll 1$, the wavepacket undergoes minimal spreading and squeezing, suggesting the potential of engineering almost nondiffracting matter-wavepackets. Thus, we showed that one can design a wavepacket robust against decoherence with significant potential for precision measurements, microscopy, and the preservation of quantum coherence.

A significant difference was observed compared to the free evolution of matter waves in one dimension, where the total acquired Gouy phase is only $\pi/4$ rad. In the present study, the matter waves evolving in one dimension acquired the total Gouy phase of $\pi/2$ rad in each interval of time, corresponding to the evolution from the minimum width (maximum squeezing) back to the same state. The Gouy phase, usually observed when any kind of wave undergoes spatial confinement, is manifested, in part, as a consequence of the squeezing of matter waves. Given the broad range of applications for squeezed states, we believe that the effect of squeezing on the Gouy phase could unlock novel applications by exploiting this phase.

The ability to engineer wavepackets with tailored Gouy phases and minimal diffraction could expand the horizon for precision measurements and quantum technologies. Future work could explore the extension of these results to more complex potentials or systems with additional degrees of freedom, as well as the experimental realization of these effects in ultracold atomic systems or optical setups.

ACKNOWLEDGMENTS

T.M.S. O Thanks CAPES (Brazil) for the financial support. L.S.M. acknowledges the Federal University of Pi-auf for providing the workspace. F. C. V. de Brito acknowledges the financial support from Horizon Europe, the European Union's Framework Programme for Research and Innovation, SEQUOIA project, under Grant Agreement No. 101070062. M.S. acknowledges a research grant 302790/2020-9 from CNPq. I.G.P. acknowledges Grant No. 306528/2023-1 from CNPq.

ETHICS DECLARATIONS

Competing interests. The authors declare no competing interests.

Appendix A: Expressions for the Gouy phase and wavepacket width far from the resonance

In the regime of low harmonic oscillator's frequency $\omega \ll \omega_0$ the expressions (5) and (7) for the wavepacket width and Gouy phase can be approximated to

$$B(t) \approx \sigma_0 \sqrt{1 + 2\gamma\omega_0 t + (1 + \gamma^2)\omega_0^2 t^2} \quad (A1)$$

$$- \frac{\sigma_0 \left[3 + 4\gamma\omega_0 t + (1 + \gamma^2)\omega_0^2 t^2 \right] t^2}{6\sqrt{1 + 2\gamma\omega_0 t + (1 + \gamma^2)\omega_0^2 t^2}} \omega^2 + \mathcal{O}(\omega^4),$$

and

$$\mu(t) \approx \frac{1}{2} \arctan \left(\frac{\omega_0 t}{1 + \gamma\omega_0 t} \right) \quad (A2)$$

$$+ \frac{\omega_0 t^3}{6 + 12\gamma\omega_0 t + 6\omega_0^2 t^2 (1 + \gamma^2)} \omega^2 + \mathcal{O}(\omega^4).$$

The first term of both expressions reproduces the free dynamics studied previously in [56], defining $\tau_0 = \omega_0^{-1}$ as the temporal analogous of the Rayleigh length.

In the regime where the natural frequency of the confining oscillator is much larger than the intrinsic frequency of the particle $\omega \gg \omega_0$ the expressions (6) and (8) for the wavepacket width and Gouy phase can be approximated to

$$B(t) \approx \sigma_0 |\cos(\omega t)| + \frac{\sigma_0 \gamma \omega_0 |\cos(\omega t)| \sin(\omega t)}{\cos(\omega t)} \frac{1}{\omega} + \mathcal{O}\left(\frac{1}{\omega^2}\right), \quad (A3)$$

and

$$\mu(t) \approx \frac{\tan(\omega t)}{2} \left(\frac{\omega_0}{\omega} \right) - \gamma \frac{\tan(\omega t)^2}{2} \left(\frac{\omega_0}{\omega} \right)^2 + \frac{(3\gamma^2 - 1) \tan(\omega t)^3}{6} \left(\frac{\omega_0}{\omega} \right)^3 + \frac{(-\gamma^3 + \gamma) \tan(\omega t)^4}{2} \left(\frac{\omega_0}{\omega} \right)^4 + \mathcal{O}\left(\frac{\omega_0}{\omega}\right)^5 \quad (A4)$$

-
- [1] L. G. Gouy, Sur une propriété nouvelle des ondes lumineuses (Gauthier-Villars, 1890).
 - [2] L. G. Gouy, *Compt. Rendue Acad. Sci. Paris* **111**, 33 (1890).
 - [3] X. Pang, T. D. Visser, and E. Wolf, *Opt. Comm.* **284**, 5517 (2011).
 - [4] X. Pang, G. Gbur, and T. D. Visser, *Opt. Lett.* **36**, 2492 (2011).
 - [5] X. Pang and T. D. Visser, *Opt. Exp.* **21**, 8331 (2013).
 - [6] X. Pang, D. G. Fischer, and T. D. Visser, *Opt. Lett.* **39**, 88 (2014).
 - [7] A. E. Siegman, *Lasers* (University science books, 1986).
 - [8] P. Balcou and A. L'Huillier, *Phys. Rev. A* **47**, 1447 (1993).
 - [9] M. Lewenstein, P. Salieres, and A. L'huillier, *Phys. Rev. A* **52**, 4747 (1995).

- [10] F. Lindner, W. Stremme, M. G. Schätzel, F. Grasbon, G. G. Paulus, H. Walther, R. Hartmann, and L. Strüder, *Phys. Rev. A* **68**, 013814 (2003).
- [11] F. Lindner, G. G. Paulus, H. Walther, A. Baltuška, E. Goulielmakis, M. Lezius, and F. Krausz, *Phys. Rev. Lett.* **92**, 113001 (2004).
- [12] V. Pablo, M. M. Oscar, and A. T. Gustavo, *Prog. In Electromag. Res.* **140**, 599 (2013).
- [13] P. Polynkin, M. Kolesik, J. V. Moloney, G. A. Siviloglou, and D. N. Christodoulides, *Science* **324**, 229 (2009), <https://www.science.org/doi/pdf/10.1126/science.1169544>.
- [14] Y.-X. Ren, H. He, H. Tang, and K. K. Y. Wong, *Frontiers in Physics* **9**, 698343 (2021).
- [15] L. Allen, M. W. Beijersbergen, R. Spreeuw, and J. Woerdman, *Physical review A* **45**, 8185 (1992).
- [16] L. Allen, M. Padgett, and M. Babiker, in *Prog. Opt.*, Vol. 39 (Elsevier, 1999) pp. 291–372.
- [17] G. Guzzinati, P. Schattschneider, K. Y. Bliokh, F. Nori, and J. Verbeeck, *Phys. Rev. Lett.* **110**, 093601 (2013).
- [18] P. Schattschneider, T. Schachinger, M. Stöger-Pollach, S. Löffler, A. Steiger-Thirsfeld, K. Y. Bliokh, and F. Nori, *Nat. Comm.* **5**, 4586 (2014).
- [19] B. P. da Silva, V. Pinillos, D. Tasca, L. Oxman, and A. Khoury, *Phys. Rev. Lett.* **124**, 033902 (2020).
- [20] R. Martínez-Herrero and F. Prado, *Optics Express* **23**, 5043 (2015).
- [21] D. Kawase, Y. Miyamoto, M. Takeda, K. Sasaki, and S. Takeuchi, *Physical review letters* **101**, 050501 (2008).
- [22] M. Hiekkamäki, R. F. Barros, M. Ornigotti, and R. Fickler, *Nature Photonics* **16**, 828 (2022).
- [23] X. Gu and M. Krenn, *Nature Photonics* **16**, 815–817 (2022).
- [24] G. Agarwal and R. Simon, *Optics communications* **100**, 411 (1993).
- [25] Y. Guo, V. D. Vaidya, R. M. Kroeze, R. A. Lunney, B. L. Lev, and J. Keeling, *Phys. Rev. A* **99**, 053818 (2019).
- [26] C. Roh, G. Gwak, and Y. Ra, *Scientific Reports* **11**, 18991 (2021).
- [27] R. Martínez-Herrero and F. Prado, *Optics Express* **23**, 5043 (2015).
- [28] M. Korobko, J. Südbeck, S. Steinlechner, and R. Schnabel, *Physical Review Letters* **131**, 143603 (2023).
- [29] Q. Wu, D. A. Chisholm, R. Muffato, T. Georgescu, J. Homans, H. Ulbricht, M. Carlesso, and M. Paternostro, *Quantum Science and Technology* **9**, 045038 (2024).
- [30] I. Pupeza, C. Zhang, M. Högner, and J. Ye, *Nature Photonics* **15**, 175 (2021).
- [31] P. Liu, J. Li, X. Li, X. Xiang, S. Wang, T. Liu, M. Cao, S. Zhang, Y. Cai, and R. Dong, *Optics Express* **32**, 42783 (2024).
- [32] I. G. da Paz, M. C. Nemes, S. Pádua, C. H. Monken, and J. G. Peixoto de Faria, *Phys. Lett. A* **374**, 1660 (2010).
- [33] I. G. da Paz, P. L. Saldanha, M. C. Nemes, and J. G. Peixoto de Faria, *New J. Phys.* **13**, 125005 (2011).
- [34] M. Arndt, A. Ekers, W. von Klitzing, and H. Ulbricht, *New J. of Phys.* **14**, 125006 (2012).
- [35] A. Hansen, J. T. Schultz, and N. P. Bigelow, in *Conference on Coherence and Quantum Optics* (Optica Publishing Group, 2013) pp. M6–64.
- [36] J. T. Schultz, A. Hansen, and N. P. Bigelow, *Optics Letters* **39**, 4271 (2014).
- [37] A. Hansen, J. T. Schultz, and N. P. Bigelow, *Optica* **3**, 355 (2016).
- [38] T. Petersen, D. Paganin, M. Weyland, T. P. Simula, S. A. Eastwood, and M. J. Morgan, *Phys. Rev. A* **88**, 043803 (2013).
- [39] T. Schachinger, S. Löffler, M. Stöger-Pollach, and P. Schattschneider, *Ultramicroscopy* **158**, 17 (2015).
- [40] R. Ducharme and I. G. da Paz, *Phys. Rev. A* **92**, 023853 (2015).
- [41] R. J. Ducharme, I. G. da Paz, and A. G. Hayrapetyan, *Physical Review Letters* **126**, 134803 (2021).
- [42] I. da Paz, R. Soldati, L. A. Cabral, J. de Oliveira Jr, and M. Sampaio, *Physical Review A* **94**, 063609 (2016).
- [43] F. de Brito, I. G. da Paz, B. Hiller, J. B. Araujo, and M. Sampaio, *Physics Letters A* **386**, 126989 (2021).
- [44] F. de Brito, I. G. da Paz, J. Araujo, and M. Sampaio, *Physical Review A* **104**, 062430 (2021).
- [45] L. S. Marinho, P. R. Dieguez, C. H. S. Vieira, and I. G. da Paz, *Scientific Reports* **14**, 12223 (2024).
- [46] D. J. Griffiths, *Introduction to Quantum Mechanics (2nd Edition)*, 2nd ed. (Pearson Prentice Hall, 2004).
- [47] D. J. Wineland, *Rev. Mod. Phys.* **85**, 1103 (2013).
- [48] R. Blatt and C. F. Roos, *Nature Physics* **8**, 277 (2012).
- [49] C. L. Degen, F. Reinhard, and P. Cappellaro, *Rev. Mod. Phys.* **89**, 035002 (2017).
- [50] F. Reiter, A. S. Sørensen, P. Zoller, and C. A. Muschik, *Nature Communications* **8**, 1822 (2017).
- [51] J. J. García-Ripoll, P. Zoller, and J. I. Cirac, *Journal of Physics B: Atomic, Molecular and Optical Physics* **38**, S567 (2005).
- [52] P. L. Knight, E. A. Hinds, M. B. Plenio, D. J. Wineland, M. Barrett, J. Britton, J. Chiaverini, B. DeMarco, W. M. Itano, B. Jelenković, C. Langer, D. Leibfried, V. Meyer, T. Rosenband, and T. Schatz, *Philosophical Transactions of the Royal Society of London. Series A: Mathematical, Physical and Engineering Sciences* **361**, 1349 (2003).
- [53] V. Dodonov, *J. Opt. B: Quantum Semiclass. Opt.* **4**, R1 (2002).
- [54] V. Dodonov and A. Dodonov, *Russ. Laser Res.* **35**, 39 (2014).
- [55] L. S. Marinho, I. G. da Paz, and M. Sampaio, *Phys. Rev. A* **101**, 062109 (2020).
- [56] F. R. Lustosa, P. R. Dieguez, and I. G. da Paz, *Phys. Rev. A* **102**, 052205 (2020).
- [57] P. P. da Silva, C. H. S. Vieira, L. S. Marinho, M. Sampaio, and I. G. da Paz, *The European Physical Journal Plus* **139**, 1042 (2024).
- [58] J. C. P. Porto, L. S. Marinho, P. R. Dieguez, I. G. da Paz, and C. H. S. Vieira, *Physica Scripta* **100**, 015111 (2024).
- [59] R. P. Feynman and A. R. Hibbs, *Quantum mechanics and path integrals*, International series in pure and applied physics (McGraw-Hill, New York, NY, 1965).
- [60] S. Feng and H. G. Winful, *Opt. Lett.* **26**, 485 (2001).
- [61] P. Martelli, M. Tacca, A. Gatto, G. Moneta, and M. Martinelli, *Optics Express* **18**, 7108 (2010).
- [62] X. Pang, G. Gbur, and T. D. Visser, *Optics letters* **36**, 2492 (2011).
- [63] P. Polynkin, M. Kolesik, J. V. Moloney, G. A. Siviloglou, and D. N. Christodoulides, *Science* **324**, 229 (2009).

- [64] T. Vetterburg, H. I. Dalgarno, J. Nylk, C. Coll-Lladó, D. E. Ferrier, T. Čížmár, F. J. Gunn-Moore, and K. Dholakia, *Nature methods* **11**, 541 (2014).
- [65] M. Butt and S. Khonina, *Micromachines* **15**, 771 (2024).